

## Electrospun Nanofiber-Coated Separator Membranes for Lithium-Ion Rechargeable Batteries

Hun Lee,<sup>1</sup> Mataz Alcoutlabi,<sup>1</sup> Jill V. Watson,<sup>2</sup> Xiangwu Zhang<sup>1</sup>

<sup>1</sup>Fiber and Polymer Science Program, Department of Textile Engineering, Chemistry and Science, North Carolina State University, Raleigh, NC 27695-8301

<sup>2</sup>Celgard LLC, 13800 South Lakes Drive, Charlotte, NC 28273

Correspondence to: X. Zhang (E-mail: xiangwu\_zhang@ncsu.edu)

**ABSTRACT:** Nanofiber-coated composite membranes were prepared by electrospinning polyvinylidene fluoride-*co*-chlorotrifluoroethylene (PVDF-*co*-CTFE) and PVDF-*co*-CTFE/polyvinylidene fluoride-*co*-hexafluoropropylene (PVDF-*co*-HFP) onto six different Celgard<sup>®</sup> microporous battery separator membranes. Application of a PVDF-based copolymer nanofiber coating onto the surface of the battery separator membrane provides a method for improving the electrolyte absorption of the separator and the separator-electrode adhesion. Peel tests showed that both PVDF-*co*-CTFE and PVDF-*co*-CTFE/PVDF-*co*-HFP nanofiber coatings have comparable adhesion to the membrane substrates. Electrolyte uptake capacity was investigated by soaking the nanofiber-coated membranes in a liquid electrolyte solution. PVDF-*co*-CTFE and PVDF-*co*-CTFE/PVDF-*co*-HFP nanofiber-coated membranes exhibited higher electrolyte uptake capacities than uncoated membranes. It was also found that PVDF-*co*-CTFE nanofiber-coated membranes have higher electrolyte uptakes than PVDF-*co*-CTFE/PVDF-*co*-HFP nanofiber-coated membranes due to the smaller diameters of PVDF-*co*-CTFE nanofibers and higher polarity of PVDF-*co*-CTFE. The separator-electrode adhesion properties were also investigated. Results showed PVDF-*co*-CTFE and PVDF-*co*-CTFE/PVDF-*co*-HFP nanofiber coatings improved the adhesion of all six membrane substrates to the electrode. © 2013 Wiley Periodicals, Inc. *J. Appl. Polym. Sci.* 129: 1939–1951, 2013

**KEYWORDS:** batteries and fuel cells; blends; coatings

Received 20 September 2012; accepted 28 November 2012; published online 3 January 2013

**DOI:** 10.1002/app.38894

### INTRODUCTION

Lithium-ion rechargeable batteries have been considered as one of the most promising candidates for large-scale power source and energy storage devices for the near future. A critical component of lithium-ion batteries is the separator. The separator provides a physical barrier between the positive and negative electrodes to prevent electrical short circuits. The separator serves as a medium for transport of ions during the charging and discharging cycles of a battery. In addition, the separator must be electrochemically inert in the battery. It is well recognized that the separator greatly influences the electrochemical performance of lithium-ion batteries.<sup>1–3</sup> Currently, polyolefin microporous membranes are the most commonly used separator for lithium-ion rechargeable batteries. However, polyolefin microporous membranes can still be improved in terms of the adhesion of separator to electrode and wettability for the higher performance of lithium-ion batteries.<sup>4–6</sup>

A variety of approaches have been used in the development of novel porous membrane separators, including phase inversion

membranes,<sup>7–10</sup> electrospun nonwoven separators,<sup>11–14</sup> inorganic composite materials,<sup>11,12–18</sup> surface-modified membranes,<sup>19–21</sup> and multilayered separators.<sup>22,23</sup> The nanofiber membranes prepared using electrospinning methods have high porosity enabling them to host a large amount of liquid electrolyte which contributes to good electrolyte retention and high ionic conductivity.

Various polymers including polyethylene oxide (PEO),<sup>24–26</sup> polyacrylonitrile (PAN),<sup>11–13,27</sup> polymethyl methacrylate (PMMA),<sup>27–29</sup> polyvinylidene fluoride (PVDF),<sup>30,31</sup> polyvinylidene fluoride-*co*-chlorotrifluoroethylene (PVDF-*co*-CTFE),<sup>32</sup> polyvinylidene fluoride-*co*-hexafluoropropylene (PVDF-*co*-HFP),<sup>13,14,28</sup> polyvinyl chloride (PVC),<sup>29,33</sup> and polyethylene glycol (PEG)<sup>26,34</sup> have been used for electrospun nanofiber membranes. Among them, PVDF copolymers, such as PVDF-*co*-CTFE and PVDF-*co*-HFP, are particularly promising due to their good affinity to the electrolyte solution and excellent electrochemical stability in lithium-ion batteries. However, most electrospun nanofiber stand-alone membranes are inherently

**Table I.** Material Type, Thickness, Porosity, and Pore Size of Membrane Separators

	Membrane material	Thickness ( $\mu\text{m}$ )	Porosity (%)	Pore size ( $\mu\text{m}$ )
Monolayer 1	PP	25	41	0.043
Monolayer 2	PP	20	41	0.040
Monolayer 3	PP	15	74	0.096
Trilayer 1	PP/PE/PP	12	38	0.026
Trilayer 2	PP/PE/PP	16	35	0.040
Trilayer 3	PP/PE/PP	14	38	0.026

weak and do not have sufficient mechanical properties to withstand the winding forces during the battery assembling process. In addition, when they are soaked in liquid electrolyte solution, they can form polymer gels and the flow properties of these gels can lead to internal short circuits and safety hazards, especially at elevated temperatures.<sup>1,2,13,35</sup> An alternative approach uses electrospinning technology to apply nanofibers onto a microporous supporting substrate which provides the required mechanical strength. The resultant composite membrane can then withstand the stresses inherent in the manufacturing process of lithium-ion batteries.

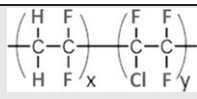
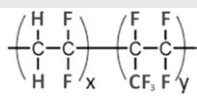
This article presents the preparation and properties of PVDF copolymer nanofiber-coated microporous membranes prepared using a nozzle-less electrospinning technique. Six different Celgard microporous polyolefin membranes were used as the supporting substrate. Electrospun PVDF copolymer nanofiber coatings were found to improve the wettability of the separator by liquid electrolyte, which is highly desirable for the development of lithium-ion batteries with high ionic conductivity and good cycling performance. The results presented in this article also demonstrate that PVDF copolymer nanofiber-coated microporous separator membranes had improved adhesion properties to the battery electrode.

## EXPERIMENTAL

### Materials

Microporous separator membranes (Celgard<sup>®</sup> LLC) were used as the base substrate for the deposition of nanofibers. To investigate the effect of substrate type on the morphology and properties of PVDF copolymer nanofiber coatings, six membrane separators, referred to as Monolayer 1, Monolayer 2, Monolayer 3, Trilayer 1, Trilayer 2, and Trilayer 3, were selected for this study. Monolayers 1 through 3 are single-layer and polypropylene (PP) microporous membranes made by using dry process technique. The trilayer microporous membranes consist of a PE monolayer membrane between two outer PP monolayers in a PP/PE/PP configuration. Table I summarizes the basic separator properties of polymer type, thickness, porosity, and pore size of the six Celgard<sup>®</sup> microporous membranes included in this study. The selected microporous membranes have pore sizes ranging from 0.026 to 0.096  $\mu\text{m}$ , thicknesses of 12–25  $\mu\text{m}$ , and porosities of 35–74%.

**Table II.** Chemical Structure, Molecular Weight, and Melting Temperature of PVDF Copolymers

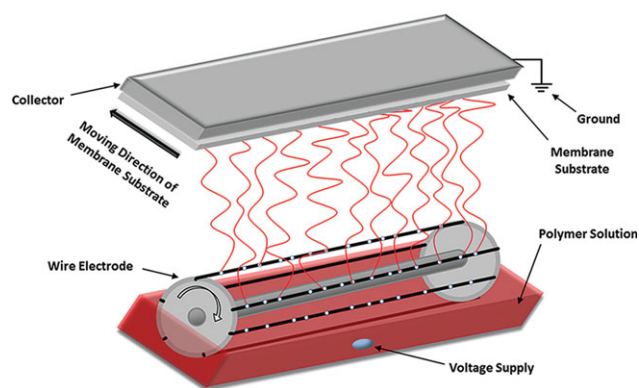
	Chemical structure	Molecular weight (g/mol)	Melting temperature ( $^{\circ}\text{C}$ )
PVDF-co-CTFE		280,000	168
PVDF-co-HFP		115,000	135

PVDF-co-CTFE (Solvay<sup>®</sup> Solef#32008) and PVDF-co-CTFE/PVDF-co-HFP (Solvay<sup>®</sup> Solef#21508) blend (9:1 by weight) dissolved in mixed solution of acetone and *N,N*-dimethylformamide (3:7 by weight) were used to prepare the electrospun nanofiber coatings. Table II shows the basic properties of the PVDF copolymers included for this study.

### Preparation of Nanofiber-Coated Separators

Nanofiber coatings were prepared by using a nozzle-less electrospinning device (NanoSpider<sup>™</sup> NS200, Elmarco), as shown in Figure 1. The electrospinning polymer solution was placed in an open solution container (not shown in Figure 1). An electrode connected with six parallel stainless steel patterned wires was rotated at a fixed speed of 6 r/min (rotation per minute) to wet the steel wires with the polymer solution. A high voltage was applied to the polymer solution to form multiple polymer jets which were ejected (up-spinning) from the solution carried on the wire surface. A 3D network of nanofibers was deposited onto the membrane substrate as it moved continuously at a fixed speed under the grounded collector. A continuous nanofiber coating with a width of 16–17 cm was deposited on the surface of the microporous membrane substrate.

The electrospinning conditions were controlled, so that nanofibers were produced having comparable morphology and uniform fiber diameters. The optimal conditions used for electrospinning

**Figure 1.** Schematic of nozzle-less electrospinning device. For simplicity, the solution container is not shown.

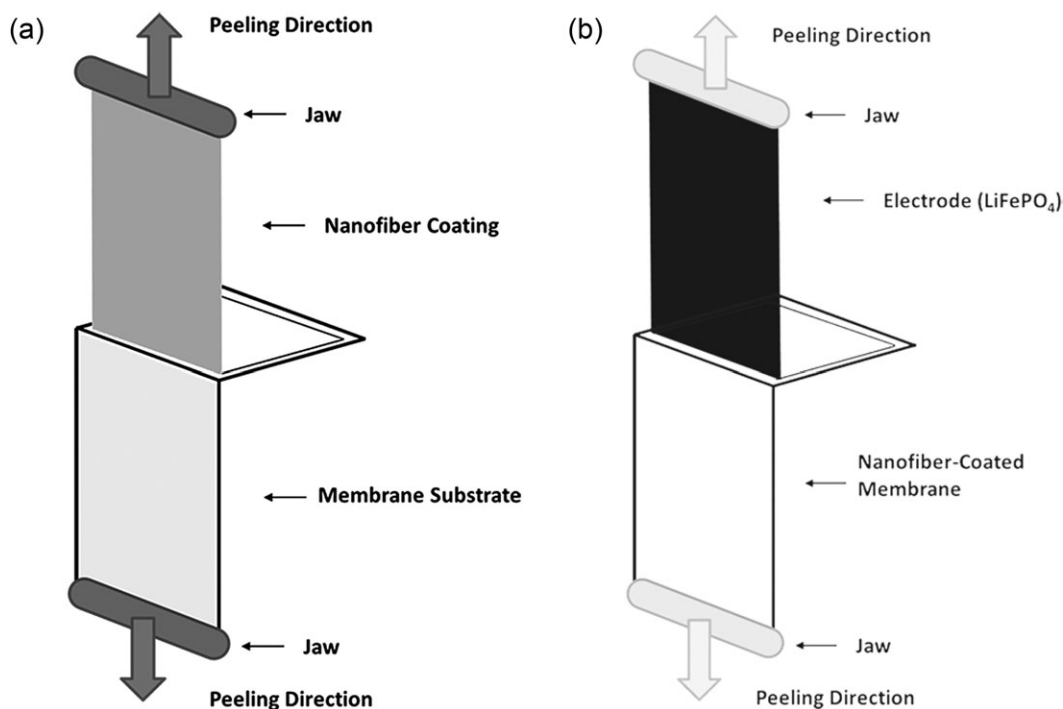


**Figure 2.** Schematic of peeling tests for measuring (a) the adhesion between nanofiber coating and membrane, and (b) the adhesion between nanofiber-coated membrane and battery electrode.

of PVDF-*co*-CTFE nanofibers were: (i) applied voltage = 40 kV, (ii) electrode-to-collector distance = 15 cm, (iii) electrode rotational speed = 6 rpm, and (iv) membrane movement speed = 0.26 m/min, while those for PVDF-*co*-CTFE/PVDF-*co*-HFP were: (i) applied voltage = 38 kV, (ii) electrode-to-collector distance = 15 cm, (iii) electrode rotational speed = 6 rpm, and (iv) membrane movement speed = 0.26 m/min. The electrospinning for PVDF-*co*-CTFE/PVDF-*co*-HFP was also carried out at 40 kV, but it did not produce uniform nanofibers. Similarly, the electrospinning for PVDF-*co*-CTFE was carried out at 38 kV, but no uniform nanofibers were obtained. Therefore, 40 kV was selected for the electrospinning of PVDF-*co*-CTFE and 38 kV was selected for PVDF-*co*-CTFE/PVDF-*co*-HFP.

#### Structure Characterization and Property Measurements

The morphology of the uncoated and nanofiber-coated membranes was evaluated using a scanning electron microscopy (JEOL 6400F Field emission SEM at 5 kV). The samples for SEM observation were pre-coated with Au/Pd by a K-550X sputter coater to reduce charging. The diameters of electrospun nanofibers were obtained by measuring fifty fibers randomly selected in SEM images using Revolution v1.6.0 software.

Liquid electrolyte uptake capacities were measured by soaking pre-weighed nanofiber-coated composite membrane samples for a fixed time at room temperature in a liquid electrolyte. The electrolyte consisted of 1 M lithium hexafluorophosphate (LiPF<sub>6</sub>) dissolved in 1:1:1 (by volume) ethylene carbonate/dimethylcarbonate/ethylmethyl carbonate. The excess electrolyte solution adhering to the surface of the composite membrane was removed by gently wiping with filter paper. The electrolyte uptake capacities were determined using the following equation:

$$\text{Uptake Capacity (mg/cm}^2\text{)} = (W_t - W_0)/A$$

where  $W_t$  was the weight of the electrolyte-immersed composite membrane,  $W_0$  the weight of dried composite membrane, and  $A$  the immersed area of the test sample.

The adhesion strength of nanofiber coatings to the membrane substrate was evaluated by using the ASTM D 1876 standard method, which is a modified ASTM D 2261 standard tongue tear test method using an Instron<sup>®</sup> Tensile Tester. Figure 2(a) depicts the modified peel test method used to evaluate the adhesion strength of nanofiber coating layer on the membrane substrate. In this method, the test was carried out on a T-type specimen of two adherends, which were the nanofiber coating and the membrane substrate, respectively. A test sample measuring  $2.5 \times 7.5 \text{ cm}^2$  was held in the two jaws of the Instron machine, with the nanofiber-coated layer clamped to the movable upper jaw and the membrane substrate attached to the fixed lower jaw. A tape (3M Scotch<sup>®</sup> Magic<sup>™</sup> Tape 810) was placed on the undersides of the nanofiber coating and the membrane substrate to prevent stretching and slipping. The jaws were set at an initial separation distance of 2.5 cm. With the upper jaw moving at a constant rate of 50 mm/min, the nanofiber coating layer was peeled away from the membrane substrate surface at a 90° angle. A 100 N load cell was used for measuring the adhesion strength of the coating layer through the entire sample length.

The adhesion between the nanofiber-coated composite membrane and a battery electrode was also evaluated by conducting peel tests on the nanofiber-coated membrane/electrode laminated assemblies, i.e., peeling the electrode away from the

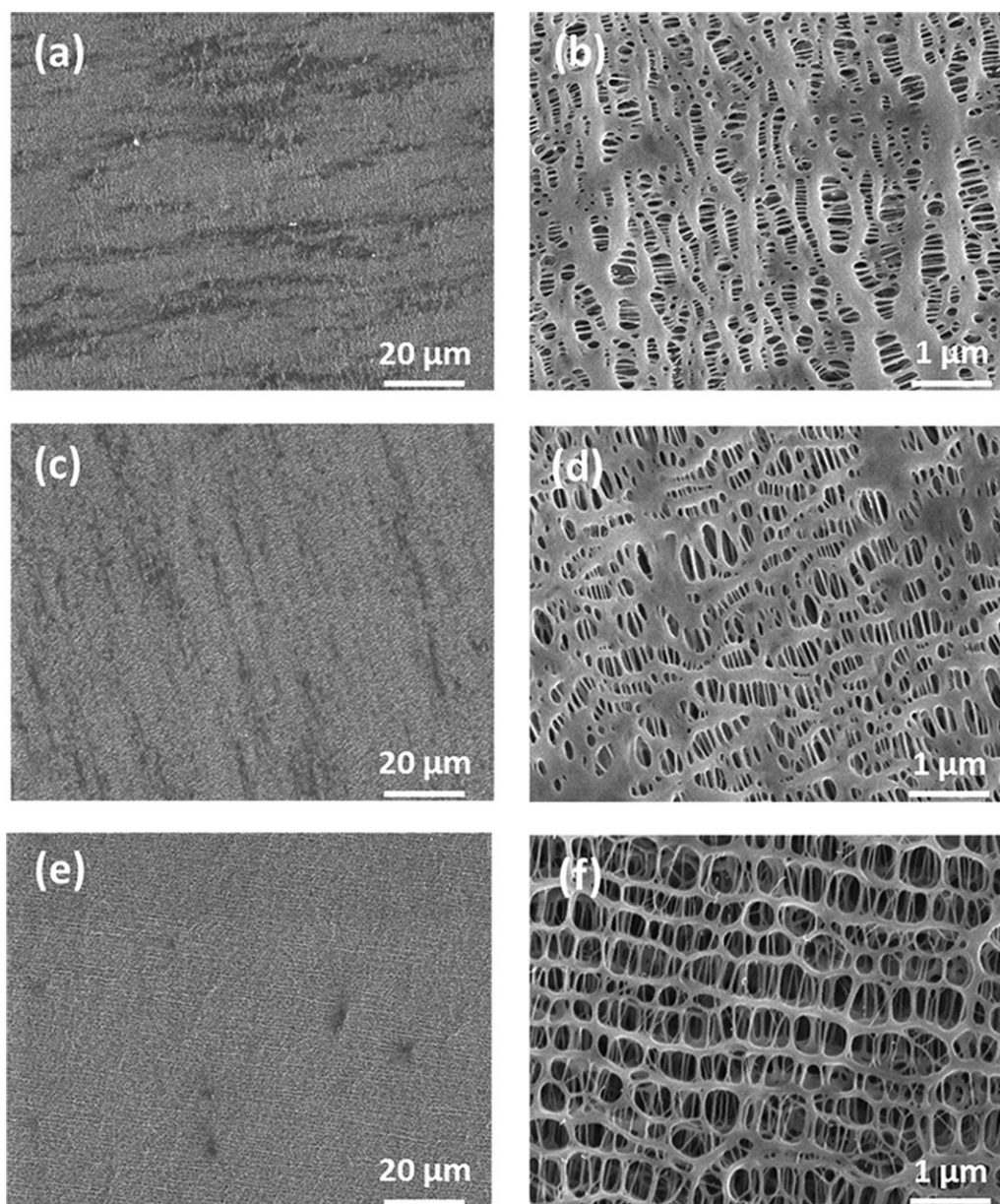


**Figure 3.** SEM images of uncoated (a,b) Monolayer 1, (c,d) Monolayer 2, and (e,f) Monolayer 3 membranes. Magnification: (a,c,e) 1,000  $\times$ , and (b,d,f) 20,000  $\times$ .

nanofiber-coated composite membrane, as shown in Figure 2(b). The electrode used was a  $\text{LiFePO}_4$  cathode (MTI Corporation). The nanofiber-coated membrane/electrode assemblies ( $2.5 \times 7.5 \text{ cm}^2$ ) were prepared by hot pressing (Carver Model C) the test sample using the press plate method at  $120^\circ\text{C}$  and 85 psi for 5 min. The peel tests were performed with a 5 N load cell. The reproducibility of electrolyte uptake capacity and adhesion results was ensured by conducting all measurements on at least eight samples.

## RESULTS AND DISCUSSION

### SEM Images

Figures 3 and 4 show SEM images of uncoated Monolayer and Trilayer membranes, respectively. All six membranes have

uniform distribution of pores with pore sizes ranging from 0.026 to 0.096. Monolayer 1 and Monolayer 2 membranes have comparable pore sizes and show typical morphology of dry process separator membranes. Monolayer 3 has unique pore structures of a different shape and size. Figure 4 shows the SEM micrographs of trilayer membranes having similar morphology, but with smaller pore sizes than those of Monolayer membranes. The six membranes were selected for this study to investigate if membrane morphology, specifically pore size, porosity, and thickness can affect the electrolyte uptake capability and the adhesion properties of electrospun nanofiber-coated microporous membranes.

It is difficult to produce nanofiber coatings with exactly the same loading density and coating thickness. However, the processing conditions were carefully controlled, so that nanofibers

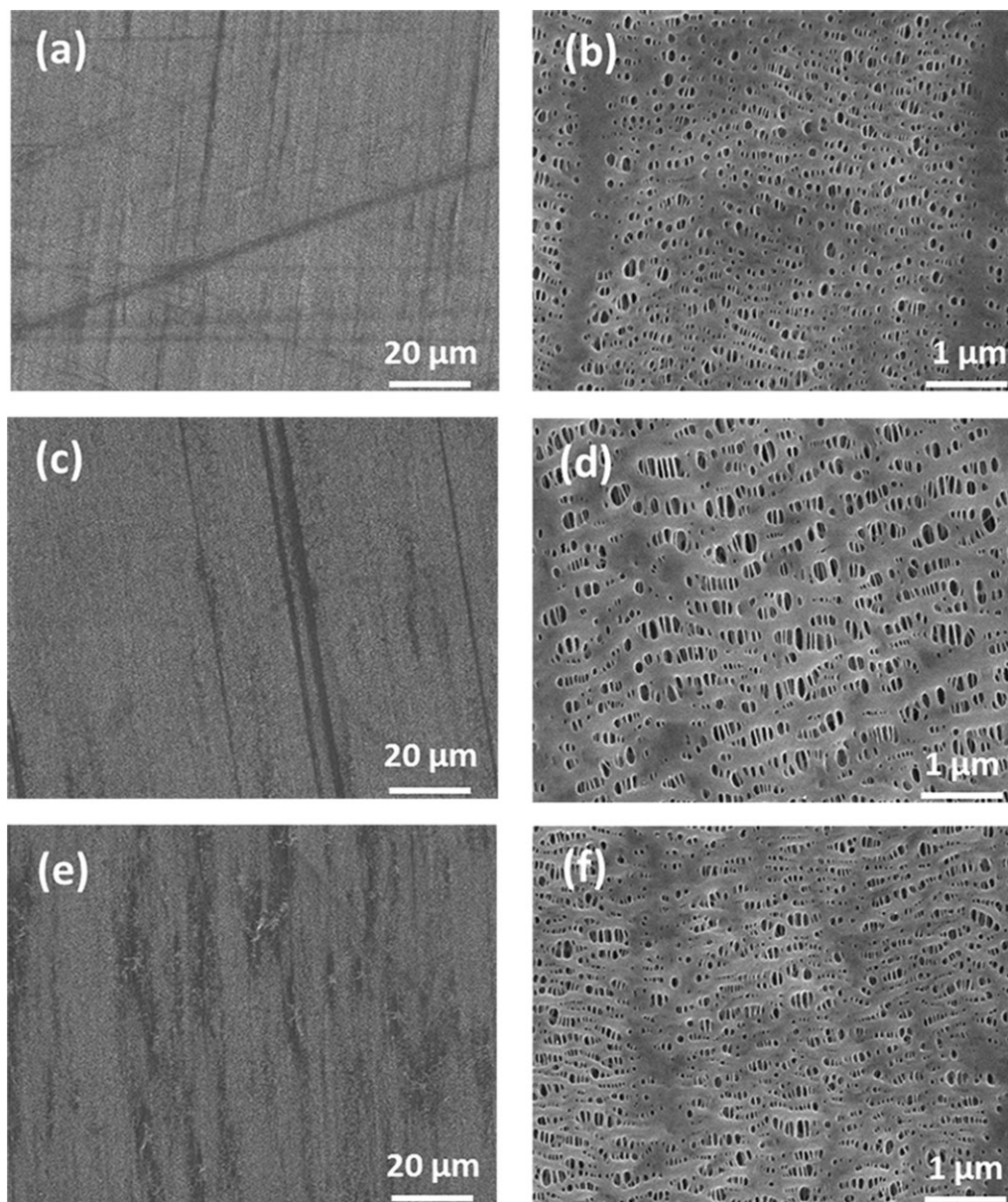


**Figure 4.** SEM images of uncoated (a,b) Trilayer 1, (c,d) Trilayer 2, and (e,f) Trilayer 3 membranes. Magnification: (a,c,e) 1,000 ×, and (b,d,f) 20,000 ×.

on the surface of membrane substrates were produced with reasonably close coating loading and thickness values. The loading densities of PVDF-*co*-CTFE nanofibers were 1.0, 0.8, 0.7, 0.7, 0.7, and 0.7 g/m<sup>2</sup> for Monolayer 1, Monolayer 2, Monolayer 3, Trilayer 1, Trilayer 2, and Trilayer 3, respectively. The loading densities of PVDF-*co*-CTFE/PVDF-*co*-HFP nanofibers were 0.9, 0.9, 0.7, 0.7, 0.8, and 0.8 g/m<sup>2</sup> for Monolayer 1, Monolayer 2, Monolayer 3, Trilayer 1, Trilayer 2, and Trilayer 3, respectively. The thicknesses of PVDF-*co*-CTFE nanofiber coatings produced on membrane substrates were 3–4, 2–4, 2–3, 2–3, 2–3, and 2–4 μm for Monolayer 1, Monolayer 2, Monolayer 3, Trilayer 1, Trilayer 2, and Trilayer 3, respectively. The thicknesses of PVDF-*co*-CTFE/PVDF-*co*-HFP nanofiber coatings produced on membrane substrates were 3–4, 3–4, 2–4, 1–3, 2–3, and 1–3 μm for Monolayer 1, Monolayer 2, Monolayer 3, Trilayer 1, Trilayer 2,

and Trilayer 3, respectively. Figures 5 and 6 show the SEM images and fiber diameter distribution of PVDF-*co*-CTFE nanofiber-coated membranes prepared by electrospinning. PVDF-*co*-CTFE nanofiber coatings on all six membrane substrates were found to have similar fiber diameters and interconnected fiber arrangement regardless of membrane type. The electrospun PVDF-*co*-CTFE nanofibers coated on both Monolayer and Trilayer membrane substrates show comparable average diameters in the range of 127–134 nm.

The SEM images and fiber diameter distribution of PVDF-*co*-CTFE/PVDF-*co*-HFP nanofiber-coated membranes are presented in Figures 7 and 8. The electrospun PVDF-*co*-CTFE/PVDF-*co*-HFP nanofibers also formed an interconnected network of randomly oriented fibers on the surfaces of both Monolayer and

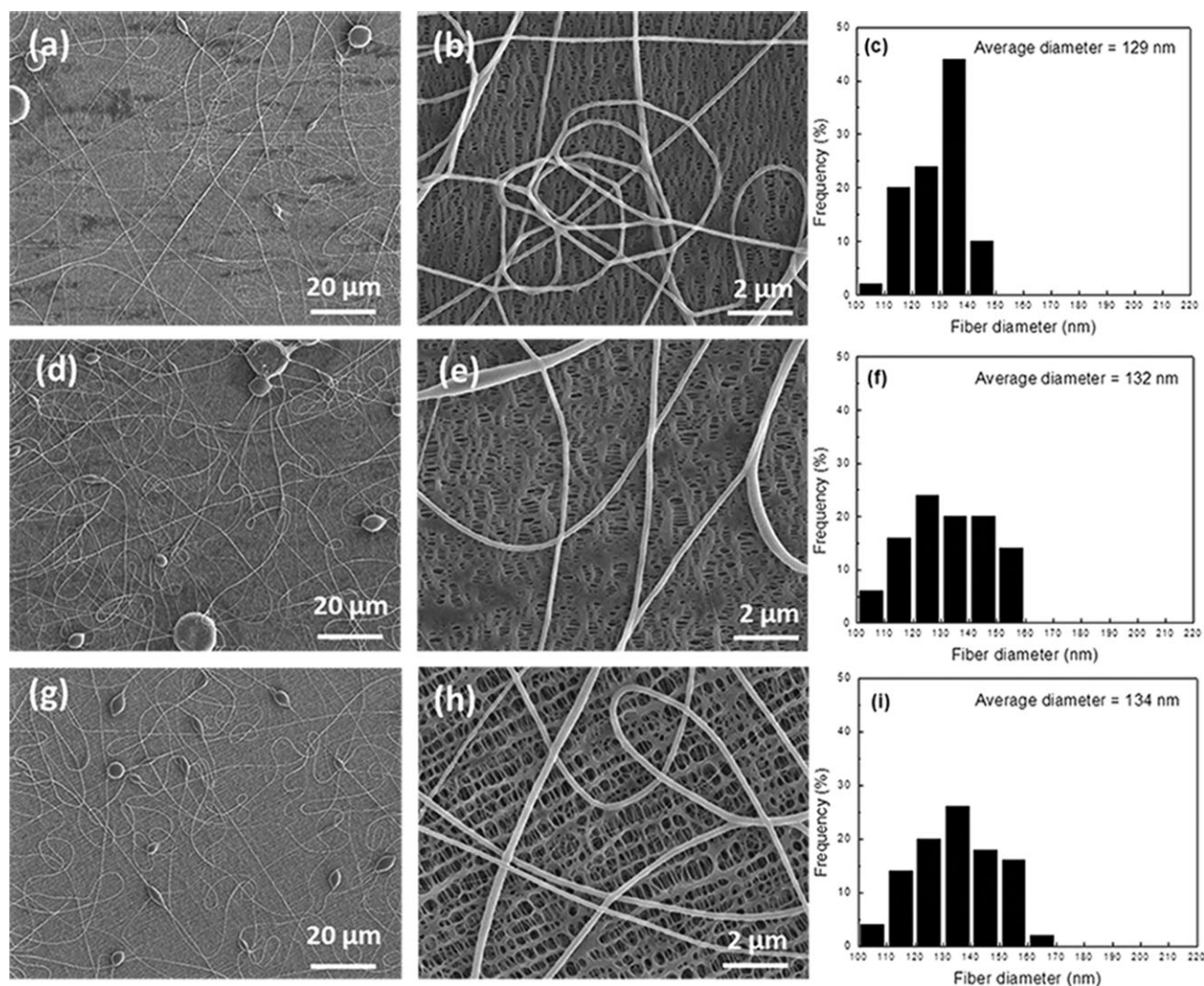


**Figure 5.** SEM images and fiber diameter distributions of PVDF-*co*-CTFE nanofiber-coated (a,b,c) Monolayer 1, (d,e,f) Monolayer 2, and (g,h,i) Monolayer 3 membranes. Magnification: (a,d,g) 1,000  $\times$ , and (b,e,h) 10,000  $\times$ .

Trilayer membrane substrates. A comparison of electrospun PVDF-*co*-CTFE nanofibers with the PVDF-*co*-CTFE/PVDF-*co*-HFP nanofibers shows that the latter has larger fiber diameters, with the average fiber diameter ranging from 165 to 183 nm. The larger fiber diameters may be attributable to the lower voltage of 38 kV used in the electrospinning of the blended PVDF-*co*-CTFE/PVDF-*co*-HFP nanofibers as compared to the 40 kV voltage used for PVDF-*co*-CTFE nanofibers.

#### Adhesion Between Nanofiber Coatings and Membrane Substrates

PVDF copolymers have been widely used as a binder for lithium-ion battery electrodes because of their excellent adhesive property.<sup>13,14,32</sup> The adhesion of the PVDF copolymer nanofibers to the base substrate membrane was investigated in this study. Peel tests were conducted on nanofiber-coated membranes to determine the adhesion force between the nanofiber coatings and the membrane substrates.

The surfaces of substrate membranes were examined by SEM after peeling off the electrospun nanofiber coatings (Figure 9). It

is seen that electrospun nanofibers were completely peeled off from the membrane substrates after the peel test. The SEM images confirm that the peeling load is determined by the adhesive property between nanofibers and membrane surface.

Figure 10(a and b) shows the loads in N/cm needed to peel the PVDF-*co*-CTFE and PVDF-*co*-CTFE/PVDF-*co*-HFP nanofiber coating layers away from the membrane substrates. Both PVDF-*co*-CTFE and PVDF-*co*-CTFE/PVDF-*co*-HFP nanofiber coatings were found to produce good adhesion to the selected membrane substrates in this study with the exception of Monolayer 3. The adhesion of electrospun nanofiber coatings on Monolayer 3 was much lower than those on other membranes. This weak adhesion may be related to the unique morphologic structure of Monolayer 3. As shown in Table 1 and Figure 3, Monolayer 3 has significantly higher porosity and larger pore size than the other membranes in this study, which resulted in a smaller contact area between the nanofibers and the membrane substrate. It is also seen in Figure 10 that the adhesions of PVDF-*co*-CTFE and PVDF-*co*-CTFE/PVDF-*co*-HFP nanofibers to membrane substrates are comparable.

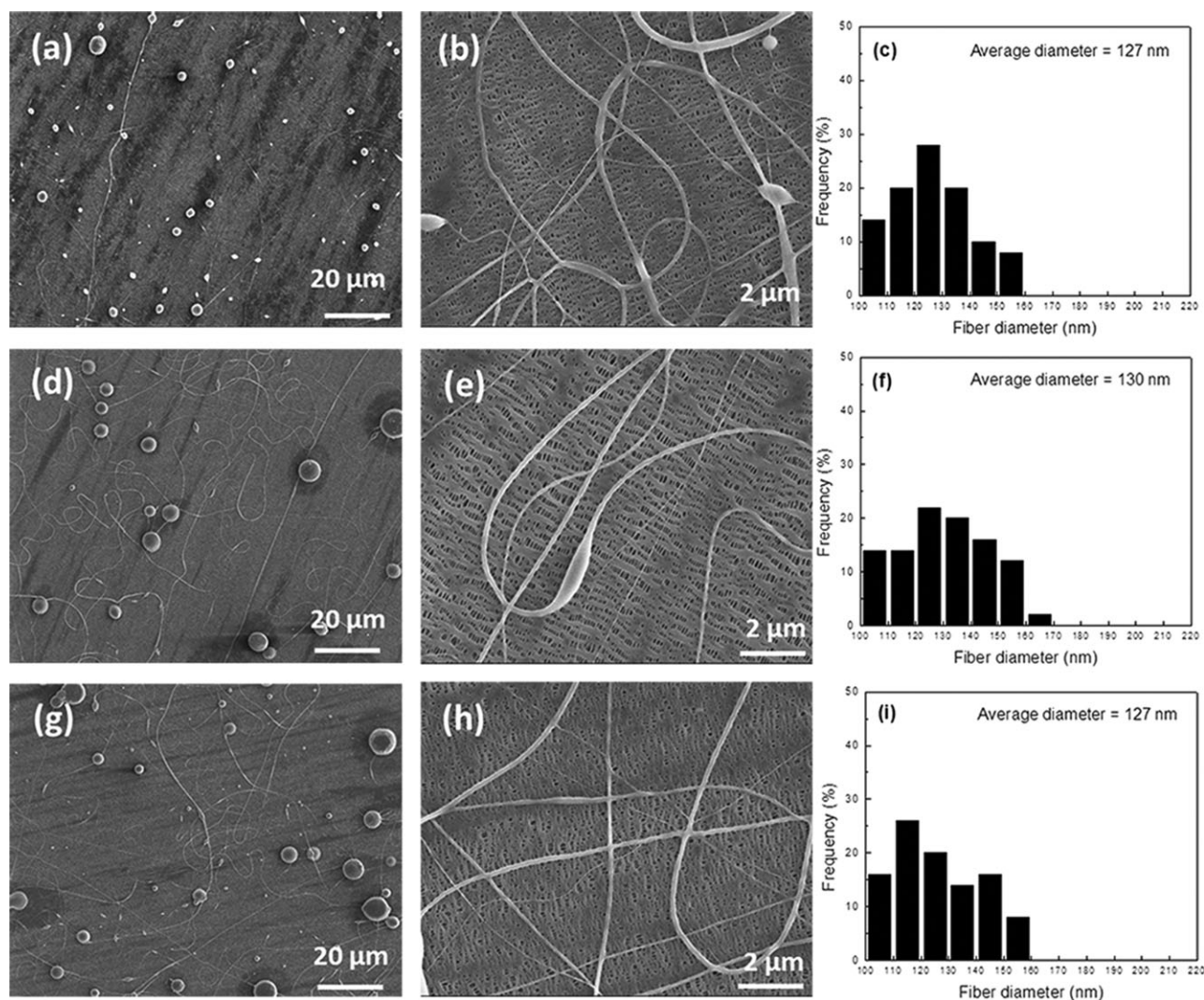


**Figure 6.** SEM images and fiber diameter distributions of PVDF-*co*-CTFE nanofiber-coated (a,b,c) Trilayer 1, (d,e,f) Trilayer 2, and (g,h,i) Trilayer 3 membranes. Magnification: (a,d,g) 1,000 ×, and (b,e,h) 10,000 ×.

### Electrolyte Uptakes of Nanofiber-Coated Membranes

Electrolyte uptake capacity is a measurement indicating the amount of liquid electrolyte solution absorbed by the unit area of a membrane separator. For lithium-ion rechargeable batteries, the separator should rapidly absorb liquid electrolyte solution to accelerate the battery assembly process and to achieve a low internal resistance and good battery performance.<sup>1,2,27</sup>

A comparison of the electrolyte uptake capacities of uncoated membranes (a), PVDF-*co*-CTFE nanofiber-coated membranes (b) and PVDF-*co*-CTFE/PVDF-*co*-HFP nanofiber-coated membranes (c) is shown in Figure 11. The absorption of liquid electrolyte was quick in the first 60 seconds, as shown in the inset of Figure 11. The electrolyte uptake capacity of membranes depends on the basic membrane properties such as thickness, porosity, and pore size. As shown in Table 1, Monolayer membranes are thicker and have higher porosity and pore size than Trilayer membranes, and hence they can have higher electrolyte capacity than that of Trilayer membranes. From Figure 11, it is seen that Trilayer 1 showed the lowest electrolyte uptake because

it has the lowest thickness and smallest pore size. On the other hand, Monolayer 3 has the highest electrolyte uptake due to its highest porosity and largest pore size in spite of thinner thickness.

Compared with uncoated membranes, electrospun PVDF-*co*-CTFE and PVDF-*co*-CTFE/PVDF-*co*-HFP nanofiber-coated membranes have higher electrolyte uptake capacities. Monolayer 1 coated with PVDF-*co*-CTFE showed better improvement in electrolyte uptake capacity than other nanofiber-coated membranes. The improvement in electrolyte uptake by nanofiber coatings should be caused mainly by the increased porosity and capillary effect on nanofibrous structure. Furthermore, PVDF-*co*-CTFE and PVDF-*co*-HFP polymers have significant amounts of polar groups and show good affinity to liquid electrolyte solutions,<sup>10,14,36</sup> leading to improved electrolyte uptakes. In this work, to investigate the effect of chemical structure of PVDF copolymer on the electrolyte uptake capacity of nanofiber coatings, PVDF-*co*-CTFE and PVDF-*co*-CTFE/PVDF-*co*-HFP blend solutions were used for the preparation of electrospun

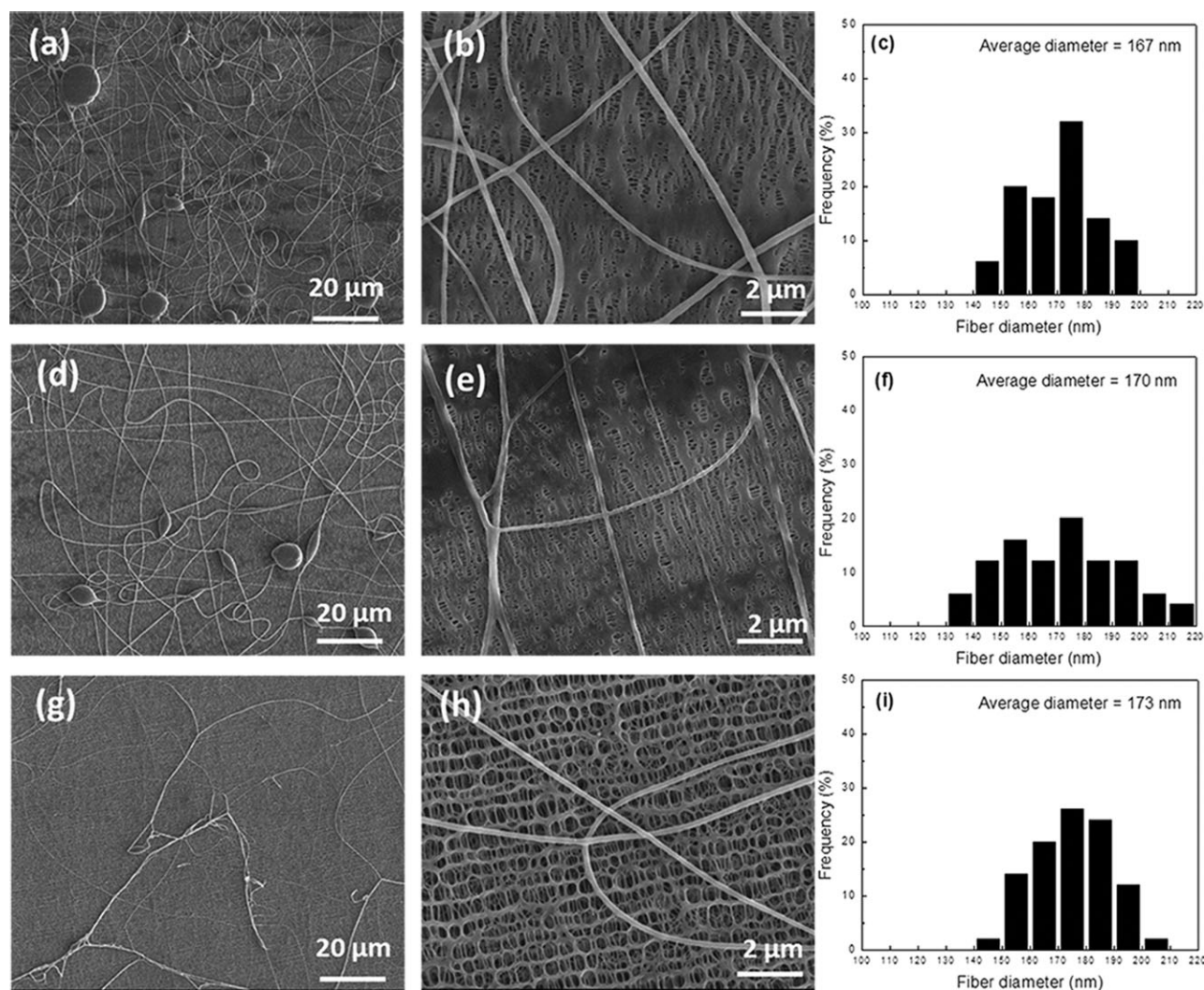


**Figure 7.** SEM images and fiber diameter distributions of PVDF-*co*-CTFE/PVDF-*co*-HFP nanofiber-coated (a,b,c) Monolayer 1, (d,e,f) Monolayer 2, and (g,h,i) Monolayer 3 membranes. Magnification: (a,d,g) 1,000  $\times$ , and (b,e,h) 10,000  $\times$ .

nanofibers on membrane substrates. Since PVDF-*co*-HFP has low molecular weight and HFP monomers on their polymer chains, they form electrospun nanofibers with lower crystallinity.<sup>14,28</sup> The initial purpose of using PVDF-*co*-CTFE/PVDF-*co*-HFP blend nanofibers was to achieve higher adsorption of liquid electrolyte solution by reducing the polymer crystallinity. However, results showed that the use of PVDF-*co*-CTFE/PVDF-*co*-HFP blend nanofibers did not improve the electrolyte uptake capacity.

The type of membrane substrate is shown to have an influence on the electrolyte uptake capacities. For example, the Trilayer membrane substrates had smaller electrolyte uptake capacities than Monolayer membrane substrates likely due to their smaller porosity and pore size (see Table I).

#### Adhesion of Nanofiber-Coated Membranes on the Electrode

Excellent adhesion between the membrane separator and the electrode is required for desirable lithium-ion battery performance. In order to evaluate the adhesive properties of nanofiber-

coated membranes to the battery electrode, PVDF-*co*-CTFE and PVDF-*co*-CTFE/PVDF-*co*-HFP nanofiber-coated membranes were laminated to a LiFePO<sub>4</sub> battery electrode to form membrane/electrode assemblies. The lamination conditions involved hot pressing the coated membranes to an electrode at 120°C and 85 psi for 5 min. Peel tests were then performed to evaluate the comparative efficacies of the PVDF-*co*-CTFE and PVDF-*co*-CTFE/PVDF-*co*-HFP nanofiber-coatings to the electrode during lamination.

Figure 12 shows the load in N/cm required to peel the PVDF-*co*-CTFE and PVDF-*co*-CTFE/PVDF-*co*-HFP nanofiber-coated membranes away from the battery electrode. For comparison, the load from the peel test of the uncoated membranes is also shown. The uncoated membranes were observed to have the lowest adhesion to the battery electrode under the test lamination conditions. The coatings of PVDF-*co*-CTFE and PVDF-*co*-CTFE/PVDF-*co*-HFP nanofibers were found to improve the adhesion between the membrane substrate and the surface of the battery electrode. The electrospun nanofiber coating layer



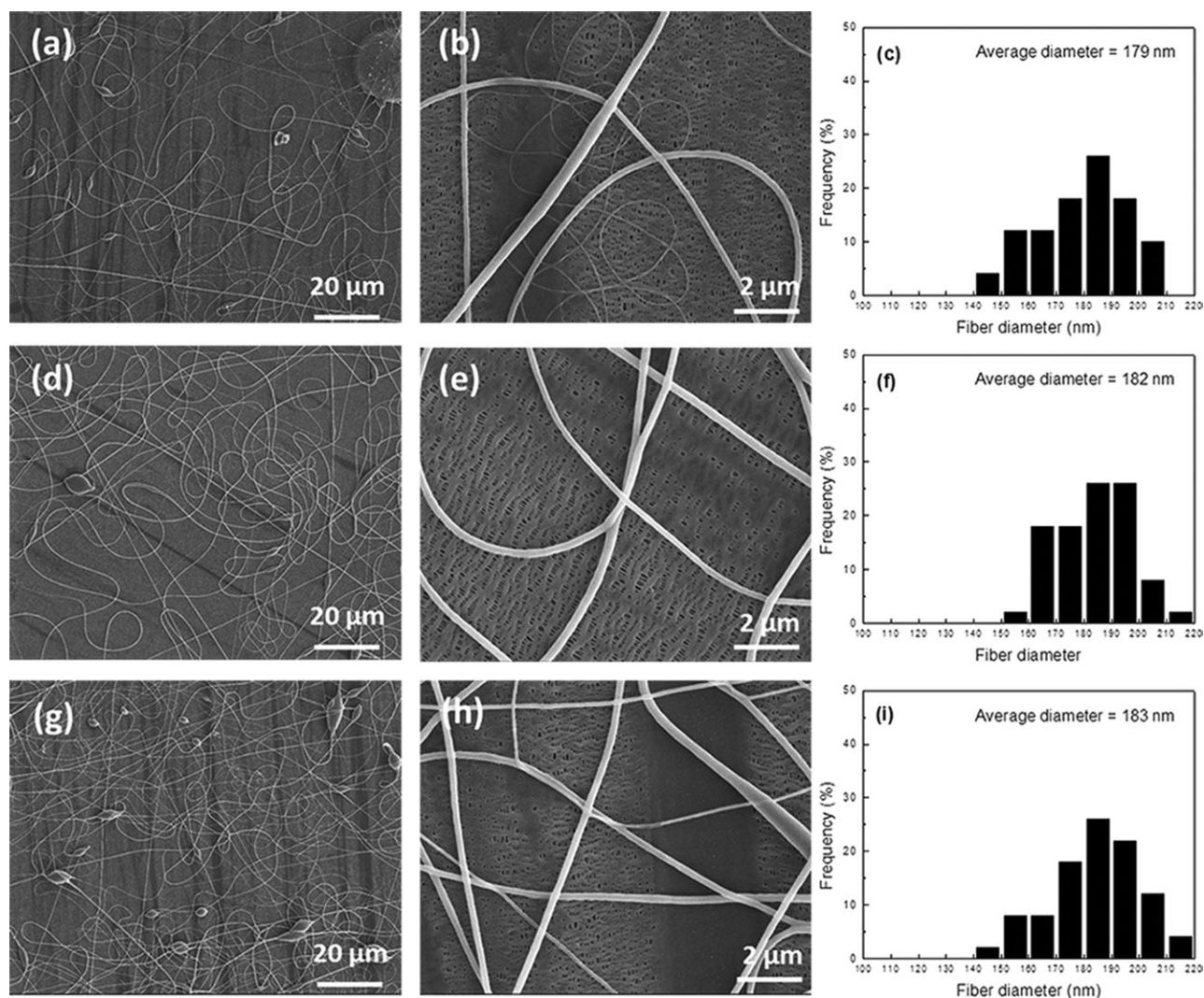


**Figure 8.** SEM images and fiber diameter distributions of PVDF-*co*-CTFE/PVDF-*co*-HFP nanofiber-coated (a,b,c) Trilayer 1, (d,e,f) Trilayer 2, and (g,h,i) Trilayer 3 membranes. Magnification: (a,d,g) 1,000 ×, and (b,e,h) 10,000 ×.

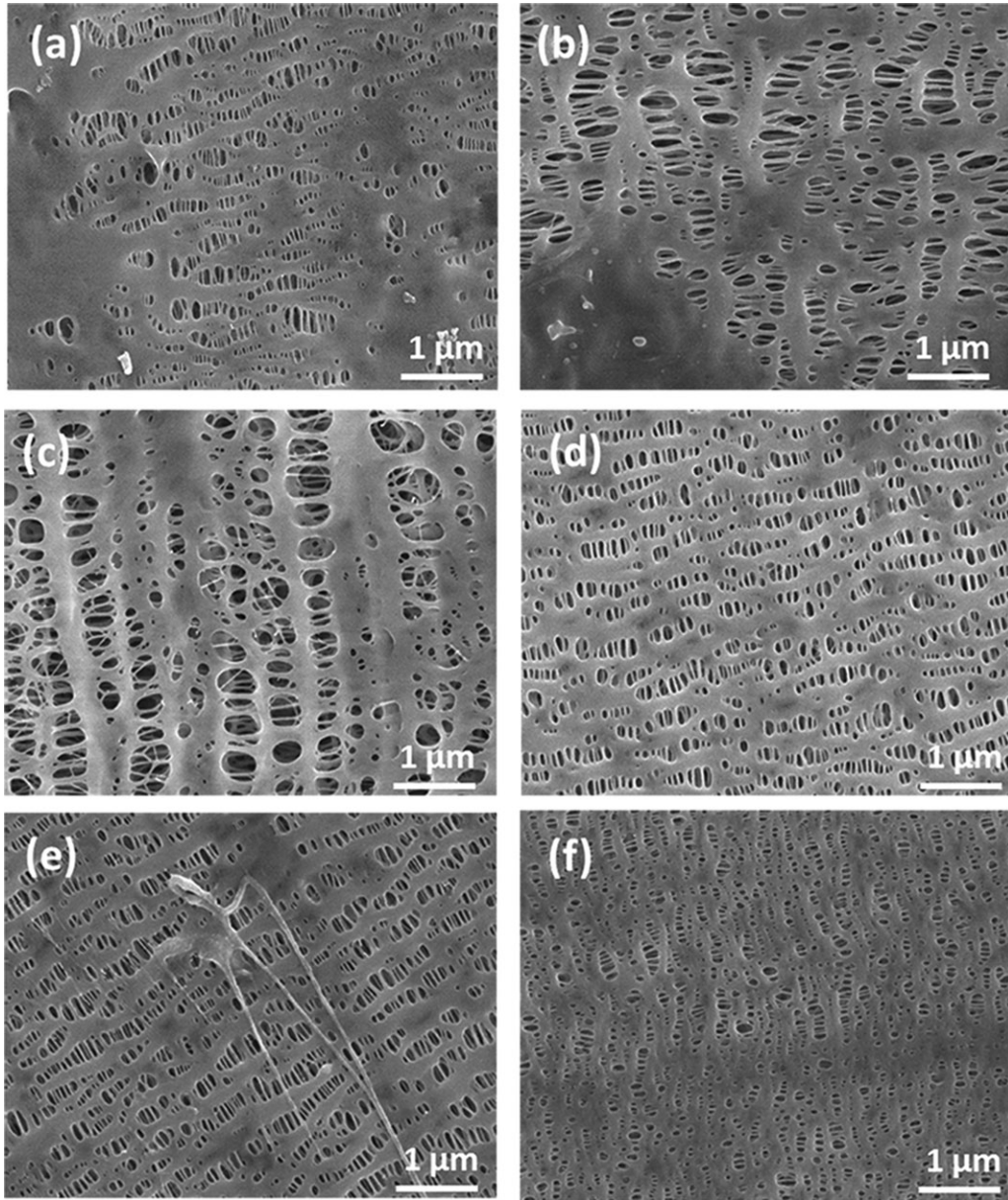
provides an effective adhesive property to bond the membrane and electrode together. As shown in Figure 12, among all samples, Monolayer 1 coated with PVDF-*co*-CTFE and PVDF-*co*-CTFE/PVDF-*co*-HFP nanofibers showed the highest separator-electrode adhesion properties. Except for Monolayer 1, nanofiber-coated Monolayer 2, Monolayer 3, Trilayer 1, Trilayer 2, and Trilayer 3 exhibited comparable peeling strength. The results demonstrate that there is no correlation between the separator-electrode adhesion and the thickness of membrane substrate. The initial purpose of using PVDF-*co*-CTFE/PVDF-*co*-HFP blend copolymer was to enhance the adhesion properties. However, it was found that the adhesion of PVDF-*co*-CTFE nanofiber-coated membranes to the electrode was higher than that of PVDF-*co*-CTFE/PVDF-*co*-HFP nanofiber-coated membranes. Therefore, using PVDF-*co*-CTFE/PVDF-*co*-HFP blend polymer solution has no improvement on the separator-electrode adhesion.

Figure 13 shows SEM images of uncoated and nanofiber-coated membranes after they were peeled off from the electrode sur-

face. After performing the peel tests, a large amount of electrode particles were moved from the electrode surface and were attached onto the nanofiber-coated membranes due to the good adhesive properties of nanofiber coatings. However, on the uncoated membrane, only a few small electrode particles were found because of the absence of nanofiber coatings. These SEM images further confirm that the adhesion between the separator membrane and the electrode has been improved by the deposition of nanofiber coatings on the membrane surface.

## SUMMARY

A nozzle-less electrospinning method was used to prepare PVDF-*co*-CTFE and PVDF-*co*-CTFE/PVDF-*co*-HFP nanofiber-coated battery separator membranes. The nanofiber composite membranes were prepared by electrospinning PVDF-*co*-CTFE and PVDF-*co*-CTFE/PVDF-*co*-HFP blended polymers onto a series of Celgard<sup>®</sup> microporous battery separator membranes. Six different types of Celgard<sup>®</sup> microporous membrane substrates were used to study the effect of substrate type on the structure and



**Figure 9.** SEM images of PVDF-*co*-CTFE nanofiber-coated (a) Monolayer 1, (b) Monolayer 2, (c) Monolayer 3, (d) Trilayer 1, (e) Trilayer 2, and (f) Trilayer 3 membranes after peel test. Magnification: 20,000 ×.

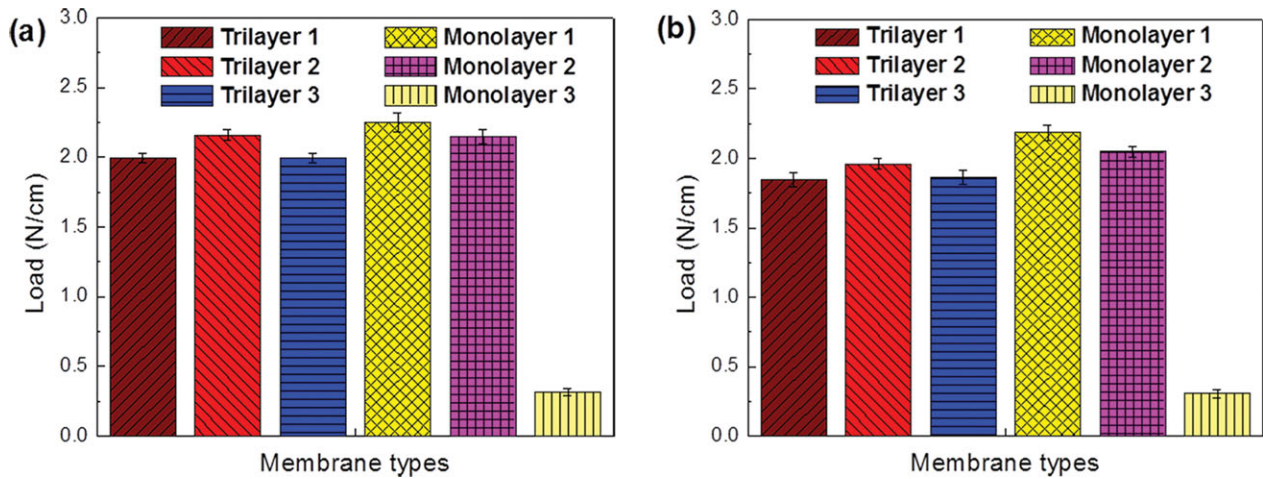


**Figure 10.** Peeling load of (a) PVDF-*co*-CTFE and (b) PVDF-*co*-CTFE/PVDF-*co*-HFP nanofiber coatings from the membrane substrates.

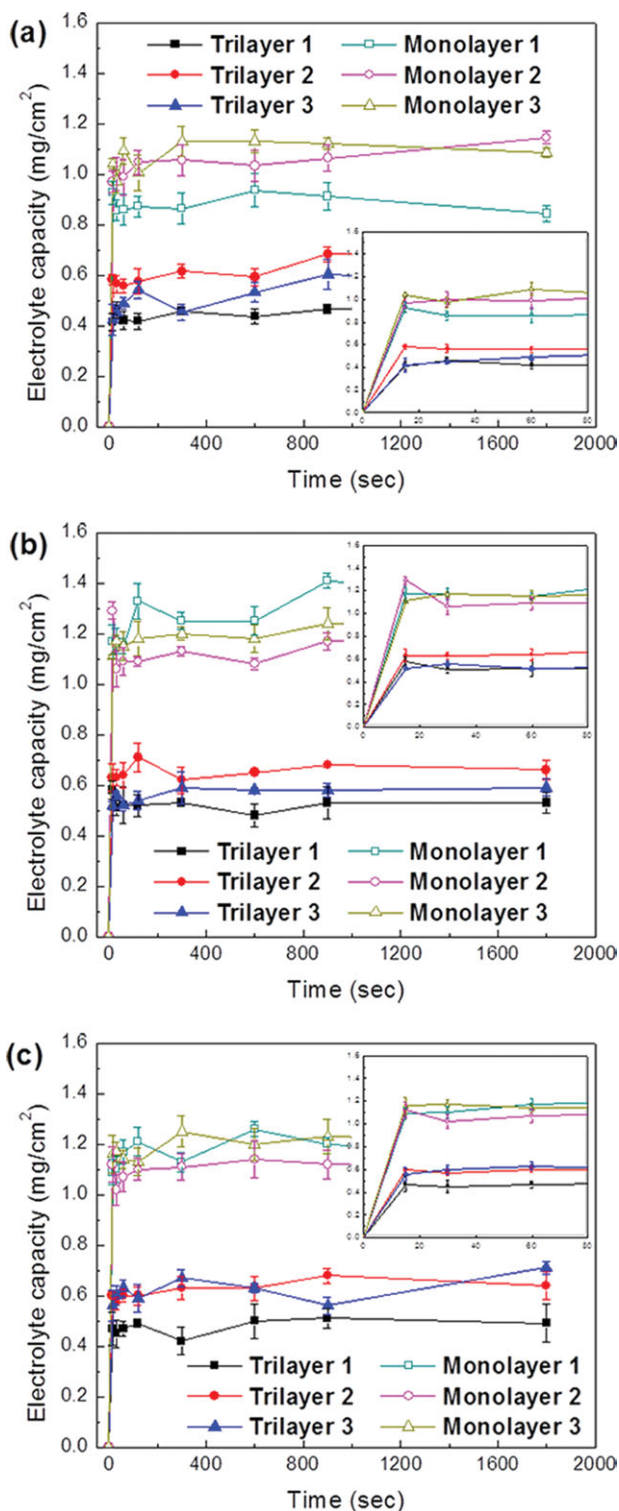


**Figure 11.** Electrolyte uptake capacity as a function of time for (a) uncoated, (b) PVDF-*co*-CTFE nanofiber-coated, and (c) PVDF-*co*-CTFE/PVDF-*co*-HFP nanofiber-coated membranes. Inset shows the uptake capacities within 60 sec.

performance properties of PVDF nanofiber coatings. Electrospun PVDF-*co*-CTFE and PVDF-*co*-CTFE/PVDF-*co*-HFP nanofiber coatings showed comparable adhesion to the membrane sub-

strates, except for Monolayer 3 which has the highest porosity and largest pore size. Electrospinning nanoscale fibrous coatings onto the surface of microporous membranes provided an effective method for improving the absorption of liquid electrolyte by the separator membranes. The improved electrolyte uptake capacity of the PVDF nanofiber-coated membranes observed in this study is due to high affinity of PVDF copolymers and the capillary effect of the electrospun nanofibers deposited on the surface of the membrane substrates. Regardless of types of microporous membrane substrate used in this study, the PVDF copolymer nanofiber coatings were found to provide improved adhesion to the LiFePO<sub>4</sub> electrode during lamination. The properties of separator membrane material did not have a significant effect on the level of electrolyte uptake capacity and separator-electrode adhesion obtained for the series of membranes studied. Based on the results, it can be concluded that the adhesion of PVDF-*co*-CTFE nanofibers to Monolayer 1 provided the strongest nanofiber coating among all samples and PVDF-*co*-CTFE nanofiber-coated Monolayer 1 presented the highest electrolyte uptake capacity and separator-electrode adhesion property.

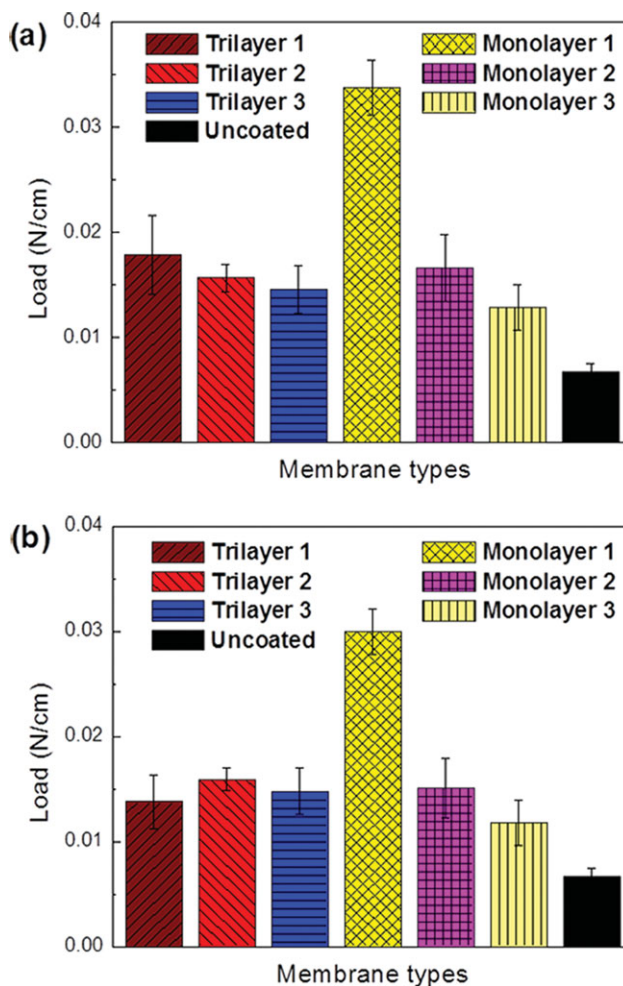


**Figure 12.** Peeling load of (a) PVDF-*co*-CTFE nanofiber-coated, and (b) PVDF-*co*-CTFE/PVDF-*co*-HFP nanofiber-coated membranes from the battery electrode. For comparison, loads for peeling uncoated membranes are also shown.

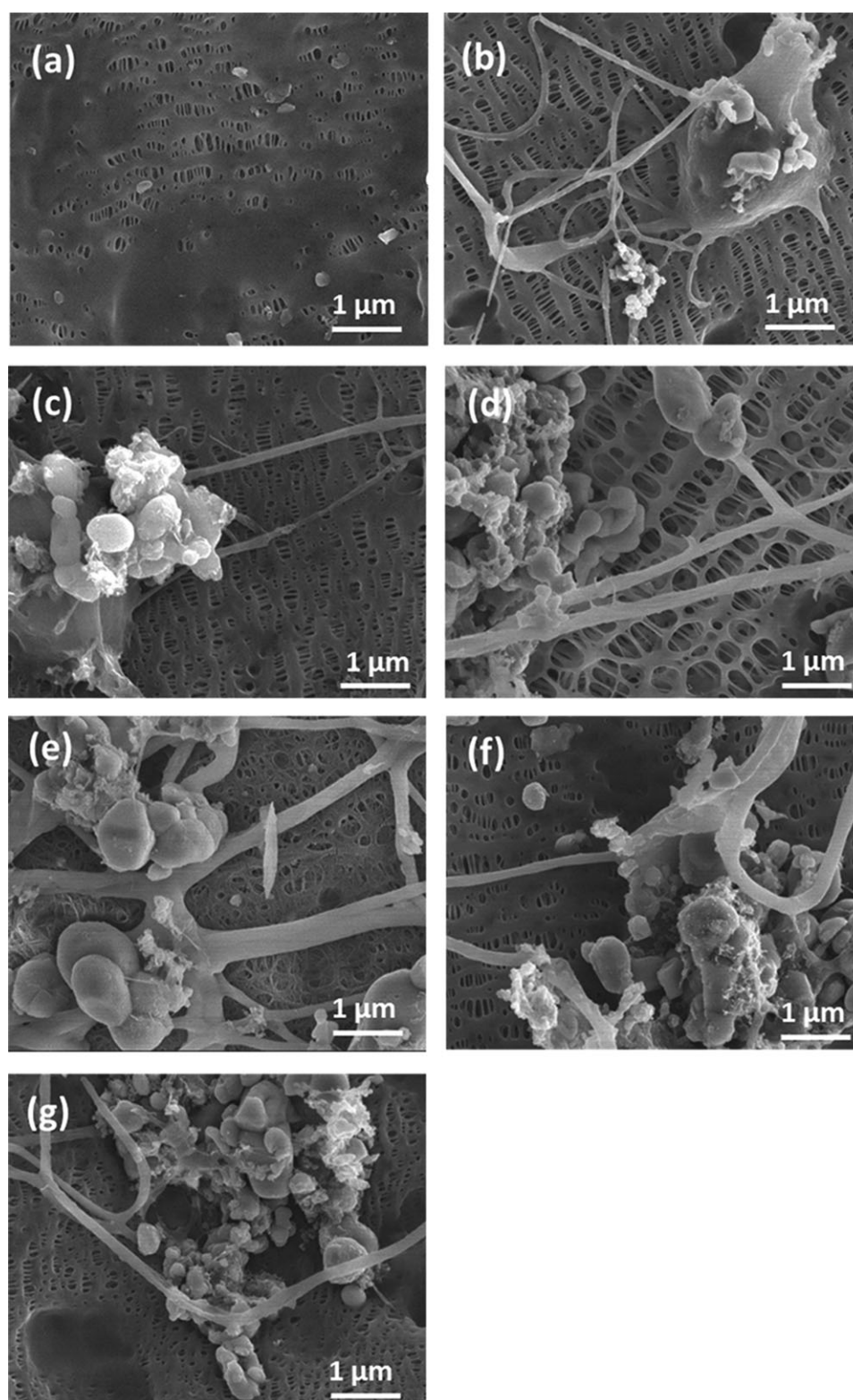


**Figure 13.** SEM images of (a) uncoated, and PVDF-co-CTFE nanofiber-coated (b) Monolayer 1, (c) Monolayer 2, (d) Monolayer 3, (e) Trilayer 1, (f) Trilayer 2, and (g) Trilayer 3 membranes after peel test. Magnification: 20,000  $\times$ .

## ACKNOWLEDGMENTS

This work was financially supported by Department of Energy (EE0002611-600). The authors acknowledge Gerald Rumierz, Lie Shi, Prem Ramadass, and Bill Paulus at Celgard LLC for their kind assistance. The authors also thank Solvay Inc. for providing PVDF copolymers.

## REFERENCES

- Winter, M.; Brodd, R. J. *Chem. Rev.* **2004**, *104*, 4245.
- Li, J.; Daniel, C.; Wood, D. J. *Power Sources* **2011**, *196*, 2452.
- Zhang, X.; Ji, L.; Toprakci, O.; Liang, Y.; Alcoutlabi, M. *Polym. Rev.* **2011**, *51*, 239.
- Djian, D.; Alloin, F.; Martinet, S.; Lignier, H.; Sanchez, J. Y. *J. Power Sources* **2007**, *172*, 416.
- Abraham, K. M.; Alamgir, M. J. *Electrochem. Soc.* **1995**, *142*, 683.
- Venugopal, G.; Moore, J.; Howard, J.; Pandalwar, S. J. *Power Sources* **1999**, *77*, 34.
- Boudin, F.; Andrieu, X.; Jehoulet, C.; Olsen, I. I. *J. Power Sources* **1999**, *81*, 804.
- Jung, B. S.; Yoon, J. K.; Kim, B. K.; Rhee, H. W. *J. Membr. Sci.* **2004**, *243*, 45.
- Du, A.; Pasquier, Warren, P. C.; Culver, D.; Gozdz, A. S.; Amatucci, G. G.; Tarascon, J. M. *Solid State Ionics*, **2000**, *135*, 249.
- Ren, Z.; Liu, Y.; Sun, K.; Zhou, X.; Zhang, N. *Electrochim. Acta* **2009**, *54*, 1888.
- Liang, Y.; Ji, L.; Guo, B.; Lin, Z.; Yao, Y.; Li, Y.; Alcoutlabi, M.; Qiu, Y.; Zhang, X. *J. Power Sources* **2011**, *196*, 436.
- Cho, T. H.; Sakai, T.; Tanase, S.; Kimura, K.; Kondo, Y.; Tarao, T.; Tanaka, M. *Electrochem Solid State Lett.* **2007**, *10*, A159.
- Bansal, D.; Meyer, B.; Salomon, M. J. *Power Sources* **2008**, *178*, 848.
- Raghavan, P.; Zhao, X.; Manuel, J.; Chauhan, G. S.; Ahn, J. H.; Ryu, H. S.; Ahn, H. J.; Kim, K. W.; Nah, C. *Electrochim. Acta* **2010**, *55*, 1347.
- Zhang, S. S.; Xu, K.; Jow, T. R. *J. Solid State Electrochem.* **2003**, *7*, 492.
- Wang, C.; Zhang, X. W.; Appleby, A. J. *J. Electrochem. Soc.* **2005**, *152*, A205.
- Wachtler, M.; Ostrovskii, D.; Jacobasson, P.; Scrosata, B. *Electrochim. Acta* **2004**, *50*, 357.
- Walkowiak, M.; Zalewska, A.; Jesionowski, T.; Waszak, D.; Czajka, B. *J. Power Sources* **2006**, *159*, 449.
- Lee, J. Y.; Bhattacharya, B.; Nho, Y. C.; Park, J. K. *Nucl. Instrum. Meth. Phys. Res. B* **2009**, *267*, 2390.
- Kim, K. J.; Kim, Y. H.; Song, J. H.; Jo, Y. N.; Kim, J. S.; Kim, Y. J. *J. Power Sources* **2010**, *195*, 6075.
- Choi, S. H.; Park, S. Y.; Nho, Y. C. *Radiat. Phys. Chem.* **2000**, *57*, 179.
- Huang, X. *J. Power Sources* **2011**, *196*, 8125.
- Kim, M.; Han, G. Y.; Yoon, K. J.; Park, J. H. *J. Power Sources* **2010**, *195*, 8302.
- Deitzel, J. M.; Kleinmeyer, J.; Harris, D.; Beck Tan, N. C. *Polymer* **2001**, *42*, 261.
- Theron, A.; Zussman, E.; Yarin, A. L. *Nanotechnology* **2001**, *12*, 384.
- Tungprapa, S.; Jangchud, I.; Ngamdee, P.; Rutnakornpituk, M.; Supaphol, P. *Mater. Lett.* **2006**, *60*, 2920.
- Rao, M.; Geng, X.; Liao, Y.; Hu, S.; Li, W. J. *Membr. Sci.* **2012**, *399*, 37.
- Ding, Y.; Zhang, P.; Long, Z.; Jiang, Y.; Xu, F.; Di, W. J. *Membr. Sci.* **2009**, *329*, 56.
- Carrozales, C.; Pelfrey, S.; Rincon, R.; Eubanks, T. M.; Kuang, A.; McClure, M. J.; Bowlin, G. L.; Macossay, J. *Polym. Adv. Technol.* **2008**, *19*, 124.
- Kim, J. R.; Choi, S. W.; Jo, S. M.; Lee, W. S.; Kim, B. C. *Electrochim. Acta* **2004**, *50*, 69.
- Choi, S. W.; Kim, J. R.; Ahn, Y. R.; Jo, S. M.; Cairns, E. J. *Chem. Mater.* **2007**, *19*, 104.
- Croce, F.; Focarete, M. L.; Hassoun, J.; Meschini, I.; Scrosati, B. *Energy Environ. Sci.* **2011**, *4*, 921.
- Lee, K. H.; Kim, H. Y.; La, Y. M.; Lee, D. R.; Sung, N. H. *J. Polym. Sci. Part B: Polym. Phys.* **2002**, *40*, 2259.
- Spasova, M.; Stoilova, O.; Manolova, N.; Rashkov, I. J. *Bioactive Compatible Polym.* **2007**, *22*, 62.
- Kritzer, P. *J. Power Sources* **2006**, *161*, 1335.
- Jeong, H. S.; Choi, E. S.; Kim, J. H.; Lee, S. Y. *Electrochim. Acta* **2011**, *56*, 5201.